Research Square

Preprints are preliminary reports that have not undergone peer review.
They should not be considered conclusive, used to inform clinical practice,
or referenced by the media as validated information.

Identification and characterization of the CCoAOMT gene family in walnut and the regulatory function of JrCCoAOMT3 in lignin biosynthesis

Ruixia Gao
Xinjiang Institute of Technology
Shangqi Yu
Tarim University
Yonglin Shao
Tarim University
Qian Ye
Tarim University
Xingyu Guo
Tarim University
Shan Gao
Tarim University
Yongqiang Chen
Tarim University
Qiang Jin
Tarim University
Rui Zhang
Tarim University
Zhongzhong Guo
15292520878@163.com
Tarim University

Research Article

Keywords: Juglans regia L., CCoAOMT gene family, lignin biosynthesis, JrCCoAOMT3, H-type lignin

Posted Date: August 20th, 2026

DOI: https://doi.org/10.21203/rs.3.rs-10506578/v1

License: This work is licensed under a Creative Commons Attribution 4.0 International License.
Read Full License

Additional Declarations: No competing interests reported.

Identification and characterization of the CCoAOMT gene family in walnut and the regulatory function of *JrCCoAOMT3* in lignin biosynthesis

Ruixia Gao[a,#], Shangqi Yu[c,#], Yonglin Shao[b,#], Qian Ye[c], Xingyu Guo[b], Shan Gao[d], Yongqiang Chen[e], Qiang Jin[e], Rui Zhang[e], Zhongzhong Guo[e,*]

a Xinjiang Institute of Technology, Aksu 843100, Xinjiang, China

b College of Horticulture and Forestry, Tarim University, Alar 843300, China.

c College of Life Science and Technology, Tarim University, Alar 843300, China.

d College of Agriculture, Tarim University, Alar 843300, China

e Southern Xinjiang Distinctive Foresty & Pomology Technology Innovation Center, Xinjiang Production and Construction Corps

# These authors contributed equally to this work.

Abstract

Background: Caffeoyl-CoA O-methyltransferase (CCoAOMT) is a key rate-limiting enzyme in plant lignin biosynthesis. Walnut (Juglans regia L.) shell hardness is largely determined by endocarp lignification, but the underlying molecular mechanism remains poorly understood.

Results: In this study, we performed genome-wide identification and systematic bioinformatics analysis of the CCoAOMT family in walnut, and verified the biological function of *JrCCoAOMT3* via heterologous overexpression in Arabidopsis thaliana (ecotype Col-0). A total of 11 JrCCoAOMT genes were identified, unevenly distributed on 5 chromosomes, all encoding proteins containing the complete conserved O-methyltransferase domain. Promoter cis-element analysis revealed abundant light-responsive and phytohormone signaling-related elements. *JrCCoAOMT3* was highly expressed during the lignification stage of walnut endocarp (peaking at PD and PE stages, 78 and 92 days after full bloom), and its encoded protein was localized in the cytoplasm. Overexpression of *JrCCoAOMT3* in A. thaliana altered stem and silique morphology, significantly increased hemicellulose content in roots and siliques, and enhanced lignin accumulation in leaves and stems. Notably, *JrCCoAOMT3* overexpression significantly reduced

* Corresponding authors:Zhongzhong Guo:

E-mail address: 15292520878@163.com

H-type lignin content across tissues, while it had no significant effect on S-type lignin and only increased G-type lignin in stems.

Conclusion: This study systematically characterizes the walnut CCoAOMT gene family and confirms the key regulatory role of *JrCCoAOMT3* in lignin biosynthesis, with a particular effect on H-type lignin monomer composition. The results provide a theoretical foundation for elucidating the molecular mechanism of walnut endocarp lignification and offer candidate gene resources for shell trait improvement.

Keywords: Juglans regia L.; CCoAOMT gene family; lignin biosynthesis; *JrCCoAOMT3*; H-type lignin

1. INTRODUCTION

Juglans regia L. (walnut) is an important woody oil and dry nut economic tree species in China, widely cultivated in Xinjiang, Yunnan and other regions, with extremely high economic value. The mechanical processing characteristics of walnut shell are key factors affecting fruit quality; excessively hard and compact shells easily cause kernel breakage during mechanical processing, while walnuts with thin shells exhibit poor stress resistance. Therefore, elucidating the molecular mechanism underlying endocarp lignification is of great significance for the genetic improvement of walnut shell traits.

Lignin is a major component of the plant cell wall, polymerized from three monomers (H, G and S), and plays critical roles in mechanical support and stress defense [3]. The content and composition of lignin directly determine wood strength and biomass utilization efficiency[52]. In the lignin biosynthesis pathway, methylation is an essential step for the formation of G-type and S-type monomers[44].

Caffeoyl-CoA O-methyltransferase (CCoAOMT) is one of the key enzymes in the lignin monomer synthesis pathway [64]. It belongs to the S-adenosyl-L-methionine-dependent O-methyltransferase family and catalyzes the methylation of caffeoyl-CoA to form feruloyl-CoA [72]. This enzyme was first confirmed to participate in lignin synthesis in studies on zinnia xylem [65]. Its discovery supplemented the lignin biosynthesis pathway and revealed two parallel methylation pathways coexisting with COMT [21].

In Arabidopsis thaliana, CCoAOMT is encoded by a small gene family [12]. Loss-of-function mutation of AtCCoAOMT1 leads to a significant reduction in lignin content, verifying its core role in lignin biosynthesis [17]. In addition, the tissue-specific member AtTSM1 participates in pollen development [14], indicating functional differentiation within this gene family. In poplar, the transcription factor PtrbZIP44-A1 cooperates with histone deacetylases to regulate the expression of PtrCCoAOMT2, thereby affecting lignin deposition [35].

In recent years, genome-wide identification of the CCoAOMT gene family has been completed in various plant species. In pomegranate, 11 CCoAOMT members are associated with seed hardness [48]; in soybean and Japanese apricot, CCoAOMT proteins are localized in the cytoplasm [18][47]. Beyond lignin synthesis, CCoAOMT also participates in biotic and abiotic stress responses, playing important roles in insect resistance in cassava [59], drought tolerance in grape [11], and fruit firmness regulation in blueberry [31].

Previous studies by our research group suggested that genes related to lignin synthesis in walnut endocarp may regulate walnut shell hardness. Based on the walnut genome database, this study systematically identified members of the CCoAOMT gene family. Combined with expression pattern analysis, subcellular localization and heterologous overexpression in A. thaliana, we further verified the function of *JrCCoAOMT3* in lignin biosynthesis. The results provide a theoretical basis and valuable candidate gene resources for the genetic improvement of walnut shell traits.

2. MATERIALS AND METHODS

2.1 Plant Materials

Samples of the 'Xinlu' walnut used in this study were collected from the Jiamu National Key Forest Improved Variety Base of Xinjiang Academy of Forestry Sciences. Sampling was performed weekly from May to July, with 30 green husk walnut fruits collected each time. The endocarp was isolated, immediately frozen in liquid nitrogen, and stored at −80 °C in an ultra-low temperature refrigerator for subsequent experiments.

The 'Xinlu' walnut samples used in this study were collected from the Jiamu National Key Forest Improved Variety Base of Xinjiang Academy of Forestry Sciences. Permission for sample

collection was obtained from the base management. The plant materials were cultivated and collected on non-protected land, and no endangered or protected species were involved in this study. All sampling procedures complied with local and national regulations.The walnut (Juglans regia L.) cultivar 'Xinlu' used in this study is a cultivated variety obtained from the Jiamu National Key Forest Improved Variety Base. As this is a cultivated variety rather than a wild species, no voucher specimen was deposited in a public herbarium. The identity of the plant material was confirmed by the base's horticultural specialists.

The wild-type A. thaliana used in this study was the Columbia-0 (Col-0) ecotype. Nicotiana benthamiana plants used for transient expression were grown under a 12 h light/12 h dark photoperiod at 25 °C for 4 weeks before infiltration.

2.2 Experimental Methods

2.2.1 Genome-Wide Identification of the Walnut CCoAOMT Gene Family

The genome annotation GFF file, CDS sequences, and protein sequences of walnut were downloaded from the walnut genome database constructed by our research group (https://walnut.ac.cn/WalnutGDB/). The whole-genome data of 'Xinlu' walnut were sequenced and published by our team [51]. The hidden Markov model (HMM) profile of the CCoAOMT conserved domain (PF01596) was retrieved from the Pfam database (http://pfam.xfam.org) [40].

The Hmmersearch program embedded in HMMER 3.0 software was used to screen candidate proteins containing the target domain with an E-value threshold of 1×10^{-10}. Meanwhile, a local BLASTP search was performed against the walnut protein dataset with the same E-value cutoff.

All candidate sequences obtained from the two approaches were integrated, and redundant sequences, incomplete open reading frames (ORFs), and poorly assembled protein sequences were eliminated. The remaining candidate proteins were further verified using Pfam and NCBI Conserved Domain Database (CDD, https://www.ncbi.nlm.nih.gov/cdd) to confirm the integrity of the conserved functional domains.

The theoretical isoelectric point (pI) and molecular weight of JrCCoAOMT proteins were predicted via ExPASy ProtParam (https://web.expasy.org/protparam/). Subcellular localization was analyzed using the online tool Euk-mPLoc 2.0

(http://www.csbio.sjtu.edu.cn/bioinf/Cell-PLoc-2/) [10].

2.2.2 Chromosomal Distribution of JrCCoAOMT Genes

Combined with BLAST alignment against A. thaliana proteins and HMMER screening in the J. regia genome, a total of 11 CCoAOMT genes were identified. Walnut genomic data were obtained from https://venyao.xyz/JuglansGDB, and A. thaliana genomic data were downloaded from Ensembl Plants (https://plants.ensembl.org/index.html).

Chromosome length statistics were calculated using the FASTA stats function in TBtools. Chromosomal localization maps were generated to visualize the physical distribution of JrCCoAOMT genes on chromosomes.

2.2.3 Phylogenetic Analysis of the JrCCoAOMT Gene Family

To explore the phylogenetic relationships and functional differentiation of JrCCoAOMT members, the CCoAOMT protein sequences of A. thaliana, Carya cathayensis Sarg., Juglans nigra L., Juglans sigillata Dode, and Engelhardia roxburghiana Wall. were selected as reference sequences.

Multiple sequence alignment was performed using MUSCLE, and a neighbor-joining (NJ) phylogenetic tree was constructed using MEGA 12 software. Bootstrap analysis with 1000 replicates was applied to evaluate topological reliability, and branches with bootstrap values greater than 50 were retained.

2.2.4 Analysis of Gene Structure, Conserved Motifs and Domains

The exon-intron structure of JrCCoAOMT genes was visualized using the online server Gene Structure Display Server (GSDS) 2.0 (http://gsds.gao-lab.org/index.php)[20].

Conserved protein motifs of JrCCoAOMTs were identified via Multiple Em for Motif Elicitation (MEME) (http://meme-suite.org/meme/tools/meme), with the maximum number of motifs set to 10. Conserved functional domains were verified using Pfam Search. All motif and domain results were integrated and visualized with TBtools.

2.2.5 Analysis of Cis-Acting Elements in JrCCoAOMT Promoters

The 2000 bp upstream promoter sequences of all JrCCoAOMT genes were extracted using TBtools. Cis-regulatory elements were predicted using the PlantCARE database (http://bioinformatics.psb.ugent.be/webtools/plantcare/html/) [24]. After manual sorting, the results were visualized with TBtools.

2.2.6 Protein Interaction Prediction and Collinearity Analysis

The protein interaction network of CCoAOMT was predicted using the STRING database (https://string-db.org), with A. thaliana selected as the reference species. Isolated nodes and non-clustered proteins were removed to optimize the network map.

Intra-genomic collinearity of walnut JrCCoAOMTs and interspecific collinearity among walnut, A. thaliana, J. nigra, and C. cathayensis were analyzed using the MCScanX module in TBtools. The results were visualized subsequently.

2.2.7 Gene Expression Profiling

Transcriptome data of walnut endocarp at different developmental stages were generated by Shenzhen Weikeom Technology Group Co., Ltd. The samples were collected from 'Xinlu' walnut fruits at ten developmental stages (PA to PF) from 50 to 140 days after full bloom (DAFB). Each stage included three biological replicates (three individual fruits from different trees). Total RNA was extracted and subjected to paired-end RNA-seq (PE150) on an Illumina platform. After quality control, reads were mapped to the walnut reference genome (GCF_001411555.2). The fragments per kilobase of transcript per million mapped reads (FPKM) values of JrCCoAOMT genes were calculated to characterize their expression patterns during lignification. A heatmap of gene expression was generated based on the normalized transcript abundance using TBtools.

The reference genome sequence and GFF annotation file used for transcriptome analysis are available at:
https://ftp.ncbi.nlm.nih.gov/genomes/all/GCF/001/411/555/GCF_001411555.2_Walnut_2.0/GCF_001411555.2_Walnut_2.0_genomic.fna.gz

https://ftp.ncbi.nlm.nih.gov/genomes/all/GCF/001/411/555/GCF_001411555.2_Walnut_2.0/GCF_001411555.2_Walnut_2.0_genomic.gff.gz

2.3 Spatiotemporal Expression and Functional Verification of Walnut *JrCCoAOMT3*

2.3.1 Primer Design for Quantitative Real-Time PCR (qRT-PCR)

The full-length coding sequence (CDS) of walnut *JrCCoAOMT3* was downloaded from NCBI. Specific qRT-PCR primers were designed using Primer 5.0 for 'Xinlu' walnut. The 18S gene was used as the internal reference.

All primers were designed with lengths of 18–25 bp, GC contents of 45%–60%, and a theoretical Tm value of approximately 58 °C. The relative expression levels of *JrCCoAOMT3* in vegetative shoots, fruiting shoots, young leaves, old leaves, exocarp, lignified endocarp, non-lignified endocarp, middle endocarp, and developing kernels were calculated using the $2^{-}\triangle\triangle Ct$ method, with vegetative shoots set as the control group.

2.3.2 Gene Cloning and Vector Construction

The full-length CDS of *JrCCoAOMT3* was amplified from walnut endocarp cDNA using specific primers. For subcellular localization analysis, the amplified CDS (without stop codon) was inserted into the pBWA(V)HS-GFP vector between the BamH I and EcoR I restriction sites to generate the 35S::*JrCCoAOMT3*-GFP recombinant vector.

For heterologous overexpression in A. thaliana, the full-length CDS of *JrCCoAOMT3* was inserted into the PHB vector between the BamH I and Pst I restriction sites using homologous recombination. All recombinant vectors were verified by Sanger sequencing (Sangon Biotech, Shanghai, China).

2.3.3 Transient Expression in Tobacco Leaves and Subcellular Localization

The verified 35S::*JrCCoAOMT3*-GFP vector and empty GFP control vector were transformed into Agrobacterium tumefaciens strain GV3101 via electroporation. The bacterial suspension was adjusted to an OD_{600} of 0.8 and infiltrated into the abaxial epidermis of

4-week-old N. benthamiana leaves using a needleless syringe.

Infiltrated plants were cultured under low light for 48 h. Leaf samples were then prepared, and the fluorescence signal was observed and photographed using a laser confocal scanning microscope.

2.3.4 Generation of *JrCCoAOMT3*-Overexpressing A. thaliana Lines

The PHB-*JrCCoAOMT3* overexpression vector was transformed into A. tumefaciens strain GV3101. Transgenic A. thaliana lines were generated using the floral dip method.

Flowering A. thaliana plants were fully watered one day before transformation. Inflorescences were immersed in the prepared Agrobacterium suspension for 30 s, and the transformation was repeated after 7 days. After 2–3 weeks, watering was reduced to promote seed maturation. Mature T_0 seeds were harvested, air-dried, and stored in a desiccator.

2.3.5 Identification of Transgenic Positive Lines

The T-DNA region of the PHB-*JrCCoAOMT3* overexpression vector contains a hygromycin resistance gene. T_0 seeds were sown on 1/2 MS medium containing 30 mg/L hygromycin for resistance screening.

Genomic DNA was extracted from resistant seedlings, with wild-type A. thaliana DNA used as the negative control. The hygromycin resistance gene was amplified by PCR to screen positive overexpression lines. The expression level of *JrCCoAOMT3* in positive lines was further detected by qRT-PCR, and homozygous T_3 lines with high expression levels were selected for subsequent phenotypic and physiological analyses.

2.3.6 Phenotypic Observation and Physiological Detection

The plant height, stem diameter, silique length, silique diameter, and silique weight of 6-week-old wild-type and *JrCCoAOMT3*-overexpressing A. thaliana plants were measured. Scanning electron microscopy (SEM) and toluidine blue staining were used to observe the anatomical structure of stems and siliques.

Total lignin and hemicellulose contents in different tissues were determined using

corresponding assay kits. Lignin monomer compositions (H/G/S units) were quantified by gas chromatography-mass spectrometry (GC-MS).

3.RESULTS

3.1 Genome-Wide Identification of the Walnut JrCCoAOMT Gene Family

A total of 11 candidate members of the JrCCoAOMT gene family were identified from the walnut genome using HMMsearch, and they were numbered from *JrCCoAOMT1* to *JrCCoAOMT11*. To further verify the relationship between their structure and function, the obtained protein sequences were analyzed and aligned with mass spectrometry data.

As shown in Table 1, among the 11 CCoAOMT proteins, the largest one was *JrCCoAOMT5* with a length of 312 amino acids, while the smallest was *JrCCoAOMT1*0 with 131 amino acids. The relative molecular weights of these proteins ranged from 14698.75 Da to 34842.43 Da, with an average of 27223.85 Da. The isoelectric points (pI) of the CCoAOMT family proteins varied from 5.01 to 8.95.

Among the 11 CCoAOMT proteins, approximately 72.73% (8 members) were hydrophilic, and 27.27% (3 members) were hydrophobic, indicating that the walnut CCoAOMT proteins are mainly hydrophilic. The results of subcellular localization prediction showed that most members of the family were distributed in the chloroplast and cytoplasm, and a few were localized in the cytoskeleton, presenting obvious characteristics of subcellular distribution differentiation.

Table 1. Basic Information and Physicochemical Properties of Walnut CCoAOMT Family Members

Gene name	No. of amino acids	Molecular weight/Da	Isoelectric poin	Instability index	Aliphatic index	Grand Average of Hydropathicity	Subcellular Localization Prediction
JrCCoAOMT1	236	26505.4	5.02	32.54	104.15	-0.075	Chloroplast
JrCCoAOMT2	247	27819.97	5.33	35.52	101.5	-0.228	Cytoskeleton
JrCCoAOMT3	247	27966.13	5.24	41.69	98.7	-0.276	Cytoskeleton、Cytoplasm

JrCCoAOMT4	235	26377.27	5.02	32.6	104.6	-0.061	Chloroplast
JrCCoAOMT5	312	34842.43	8.95	45.01	99.01	-0.023	Chloroplast
JrCCoAOMT6	236	26318.32	5.03	36.75	101.65	-0.099	Cytoplasm
JrCCoAOMT7	236	26270.62	5.48	35.39	106.19	-0.021	Cytoplasm
JrCCoAOMT8	254	28470.12	5.91	35.44	106.34	0.027	Chloroplast
JrCCoAOMT9	252	28117.81	5.35	38.86	105.24	0.033	Chloroplast
JrCCoAOMT10	131	14698.75	5.01	40	98.24	-0.063	Cytoplasm
JrCCoAOMT11	288	32075.47	5.49	38.96	110	0.107	Cytoplasm

3.2 Phylogenetic and gene structure analysis of JrCCoAOMT

To elucidate the evolutionary relationships of the walnut CCoAOMT family, multiple sequence alignments were performed on the amino acid sequences of CCoAOMT proteins from A. thaliana, walnut (J. regia), black walnut (J. nigra), hickory (C. cathayensis), iron walnut (J. sigillata), and yellow walnut (E. roxburghiana). A phylogenetic tree was constructed (Figure 1). Based on homology, the 45 CCoAOMT members were divided into eight subfamilies. The results in Figure 1A show that the six species clustered into eight subgroups (Group I to Group VIII). Groups VIII and VII contained the fewest members, with two AtCCoAOMT and two JsCCoAOMT members, respectively. Group V contained the most members, with three JrCCoAOMT members, suggesting that Group V may be the primary subfamily driving the evolution of the walnut CCoAOMT family. In addition, Groups I and IV contained multiple JrCCoAOMT members together with members from other species, indicating high homology between these two subfamilies, though further analysis is needed to clarify their exact relationships. The two CCoAOMT genes from A. thaliana formed a separate clade, indicating significant evolutionary divergence among distantly related species. Similarly, *JsCAMT9* from iron walnut formed an independent branch, suggesting that this gene has undergone notable functional divergence during evolution.

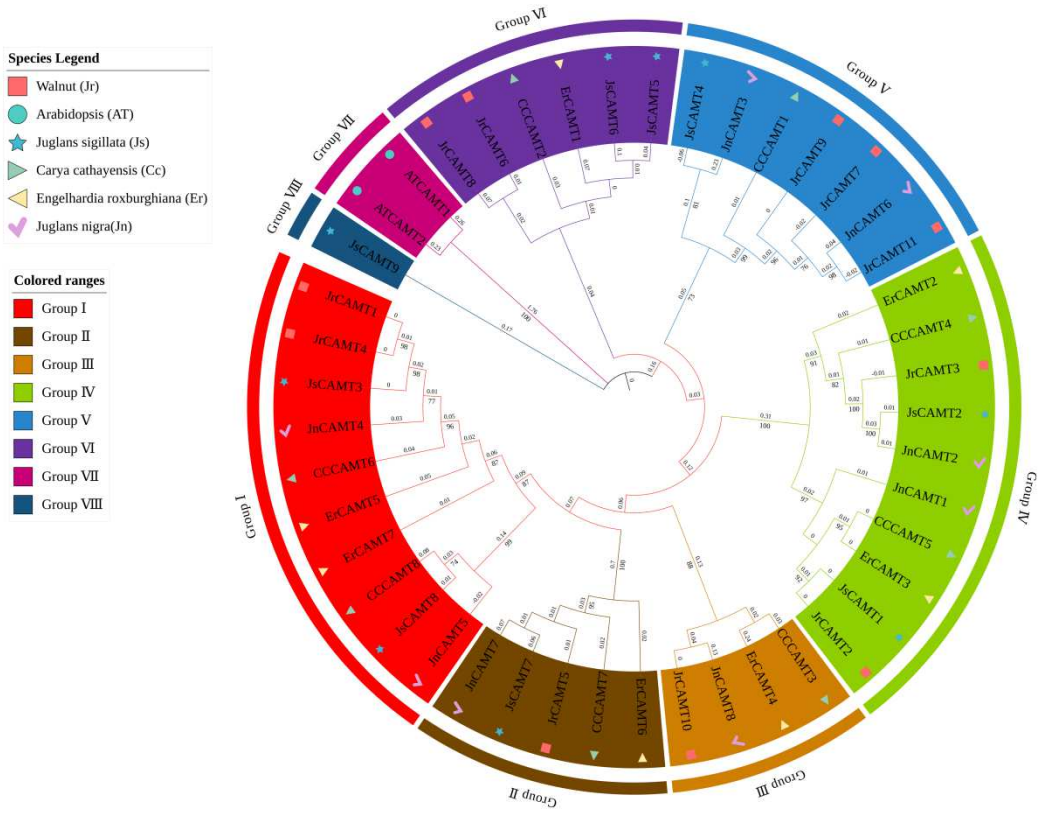


Fig. 1 Phylogenetic analysis of CCoAOMT proteins from walnutand and related species.
Multiple sequence alignment of full-length CCoAOMT amino acid sequences was performed using ClustalW. The phylogenetic tree was constructed by the neighbor-joining (NJ) method with 1000 bootstrap replicates using MEGA 11 software. Numbers on the branches indicate bootstrap support values. Different colored branches represent eight distinct phylogenetic groups (Group I to Group VIII). Different symbols correspond to different species: red square, walnut (Juglans regia, Jr); cyan circle, Arabidopsis thaliana (AT); blue star, iron walnut (Juglans sigillata, Js); green triangle, hickory (Carya cathayensis, Cc); yellow inverted triangle, yellow walnut (Engelhardia roxburghiana, Er); purple checkmark, black walnut (Juglans nigra, Jn).

Chromosomal localization analysis of the 11 JrCCoAOMT family genes showed that they are unevenly distributed on five chromosomes (Figure 2). Chromosome 10 contained the largest number of JrCCoAOMT members, with five genes clustered on this chromosome, followed by chromosome 13 with three JrCCoAOMT genes. Chromosomes 1, 9, and 16 contained the fewest members, each with only one JrCCoAOMT gene.

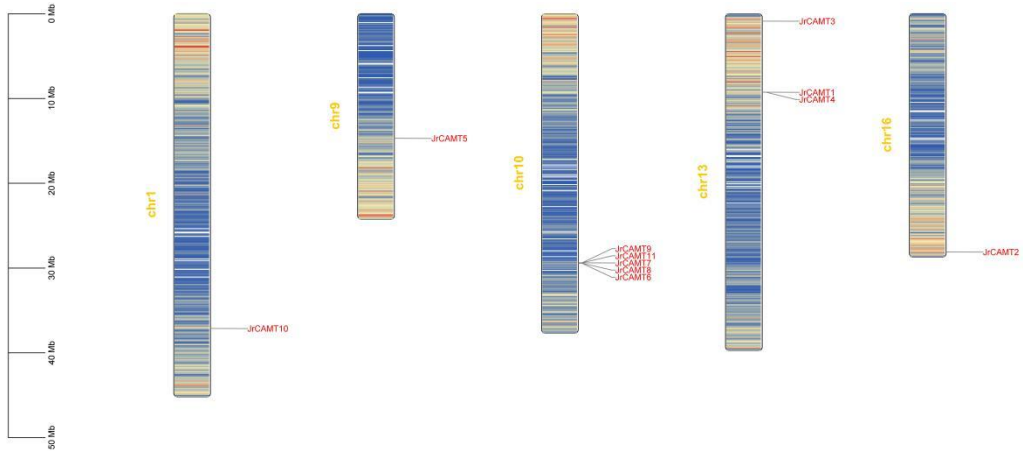


Fig. 2 Chromosomal distribution of JrCCoAOMT genes in the walnut genome.

The physical positions of JrCCoAOMT genes were mapped to the Juglans regia reference genome using TBtools v1.120 software. The vertical scale on the left indicates the physical length of chromosomes in megabases (Mb). Chromosome numbers are labeled in yellow on the left side of each chromosome. The JrCCoAOMT genes (abbreviated as JrCAMT in the figure) are marked in red on their corresponding chromosomal positions. A total of 11 JrCCoAOMT genes were unevenly distributed on 5 out of 16 walnut chromosomes.

3.3 Gene structure, protein motif, and conserved domain analysis of JrCCoAOMT

To clarify the gene structure of JrCCoAOMT, the candidate sequences of 11 walnut CCoAOMT genes were analyzed (Figure 3A). Based on phylogenetic tree clustering, the gene structures of the JrCCoAOMT family were divided into three groups: I, II, and III.

The diversity of gene structures promotes the evolution of gene families. The MEME software was used to identify conserved motifs in the JrCCoAOMT protein sequences to further explore the similarity and diversity of motifs among various walnut JrCCoAOMT proteins (Figure 3A). A total of 10 relatively conserved motifs (named Motif 1–10) were identified, which were classified into Groups I, II, and III according to the phylogenetic tree. In Group I, six conserved motifs (Motif 3, 6, 2, 5, 1, and 4) were identified. In Group II, *JrCCoAOMT1*0 contained three conserved sequences: Motif 3, Motif 1, and Motif 4. In Group III, *JrCCoAOMT5* contained six conserved motifs. In summary, Motif 5 and Motif 1 were the most conserved and stable, present in all groups. The majority of JrCCoAOMT proteins contained Motif 5, Motif 1, and Motif 4, indicating that the conserved sequences identified exhibit certain specificity.

Additionally, the intron/exon structures of the JrCCoAOMT genes were shown (Figure 3B). Genes within the same subfamily shared similar gene structures, while distinct differences were observed among different subfamilies. The results showed that in Group I, three JrCCoAOMT

genes contained five introns, and six genes contained four introns. In Group II, *JrCCoAOMT10* had one intron. In Group III, *JrCCoAOMT5* had eight introns, presumably with five exons and four introns as the main structural pattern. The gene structures of JrCCoAOMT within the same subfamily were relatively conserved.

Conserved domain analysis showed that all 11 members of the walnut CCoAOMT gene family contained a complete O-methyltransferase domain (PF01596) and no other conserved domains were detected. This single-domain composition is a typical feature of the CCoAOMT family, distinguishing it from other methyltransferase families and providing a structural basis for the conserved function of these family members in lignin biosynthesis (Figure 3C).

Cis-acting elements can reflect, to some extent, the transcriptional regulation of genes. The PlantCARE web tool was used to predict cis-acting elements in the 2000 bp upstream sequence of the start codon, and visualization was performed using TBtools software (Figure 3D). The cis-acting elements in the promoter regions of walnut JrCCoAOMT family members are shown. Based on their functions, these cis-acting elements can be divided into two major categories: hormone-responsive elements and light-responsive elements, indicating that walnut JrCCoAOMT family members may play roles in plant hormone regulation and light response.

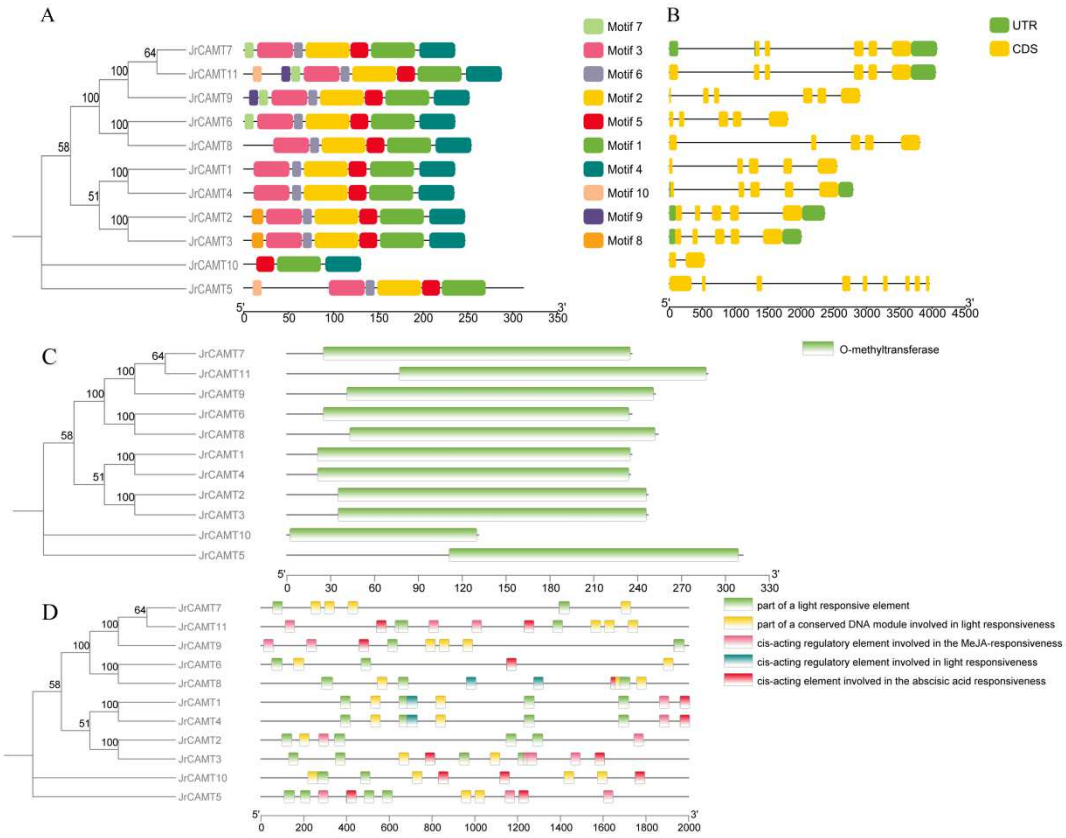


Fig. 3 Conserved motifs, gene structures, conserved domains and cis-acting elements of JrCCoAOMT genes. (A) Conserved motifs of JrCCoAOMT proteins predicted by MEME software. Different colored boxes represent 10 distinct conserved motifs, and the scale bar indicates the length of amino acid sequences. (B) Gene structures of JrCCoAOMT genes. Yellow boxes represent coding sequences (CDS), green boxes represent untranslated regions (UTR), and the scale bar indicates the length of genomic sequences. (C) Conserved domain analysis of JrCCoAOMT proteins. Green boxes represent the conserved O-methyltransferase domain, and the scale bar indicates the length of amino acid sequences. (D) Prediction of cis-acting elements in the 2000 bp upstream promoter regions of JrCCoAOMT genes. Different colored boxes represent different types of cis-acting elements, including light-responsive elements, methyl jasmonate (MeJA)-responsive elements and abscisic acid (ABA)-responsive elements. The phylogenetic trees on the left of each panel were constructed based on the full-length amino acid sequences of JrCCoAOMT proteins using the neighbor-joining method with 1000 bootstrap replicates.

3.4 Synteny analysis of JrCCoAOMT genes

To further explore the evolutionary mechanisms of the species, this study analyzed duplication events of the 11 JrCCoAOMT genes using the MCScanX program in TBtools. A total of four segmentally duplicated genes were identified. Synteny analysis (Figure 4A) indicated that segmentally duplicated genes were present on chr13, chr16, chr1, and chr10, while no JrCCoAOMT segmental duplications were found on other chromosomes. Both tandem and segmental duplications occurred during the evolution of JrCCoAOMT. Two tandem duplication events were detected: *JrCCoAOMT1* and *JrCCoAOMT4* are tandemly duplicated on chromosome 13; *JrCCoAOMT6*, *JrCCoAOMT7*, *JrCCoAOMT8*, *JrCCoAOMT9*, and *JrCCoAOMT11* are tandemly duplicated on chromosome 10. Additionally, two segmental duplication events were detected: *JrCCoAOMT1*0 with *JrCCoAOMT7*, and *JrCCoAOMT3* with *JrCCoAOMT2*.

To further explore the evolutionary relationships of JrCCoAOMT genes among different species, synteny analysis was performed using black walnut (J. nigra), hickory (C. cathayensis), and A. thaliana (Figure 4B). The results showed that walnut exhibited syntenic relationships with black walnut, hickory, and A. thaliana, with 10, 10, and 4 syntenic JrCCoAOMT genes, respectively. Among them, only four JrCCoAOMT genes (*JrCCoAOMT1*, *JrCCoAOMT3*, *JrCCoAOMT1*0, and *JrCCoAOMT7*) did not have homologous relationships in black walnut, hickory, and A. thaliana simultaneously.

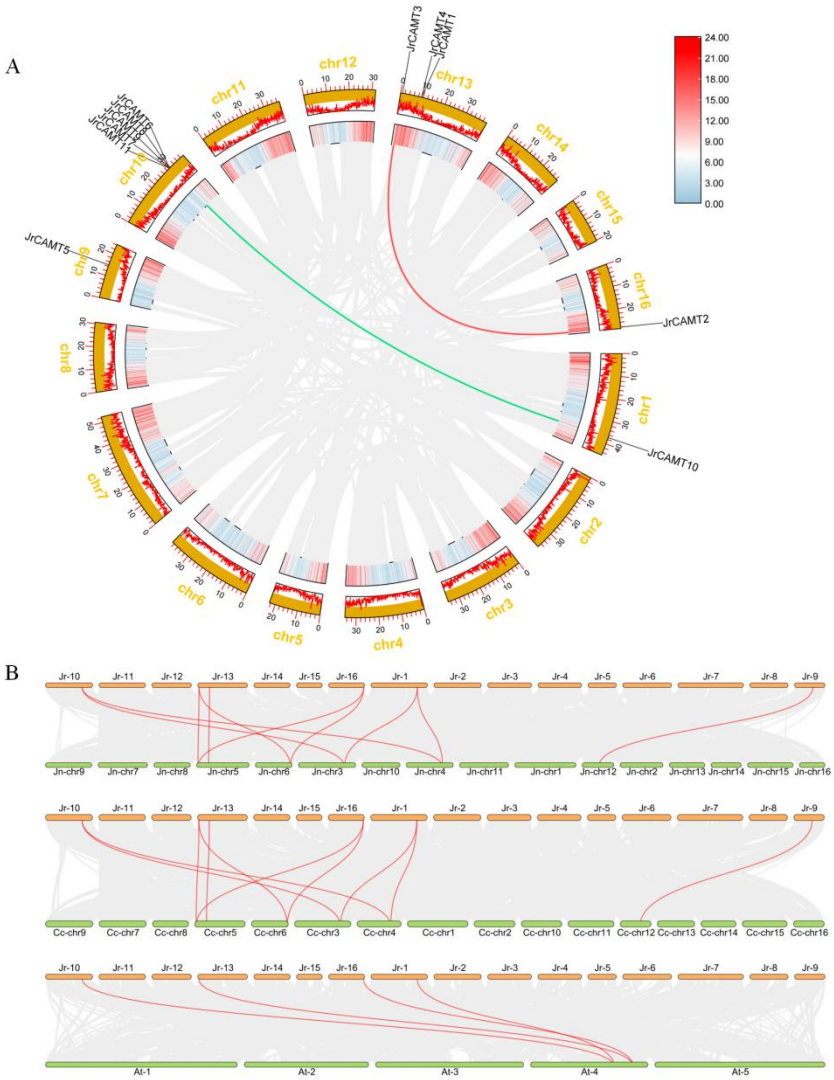


Fig. 4 Intraspecific and interspecific synteny analysis of the CCoAOMT gene family.
(A) Intraspecific synteny analysis of CCoAOMT genes in the walnut (*Juglans regia*) genome. The colored blocks represent the 16 walnut chromosomes, and the color scale on the top right indicates the gene density (genes per Mb). Gray lines represent all syntenic gene pairs in the walnut genome, while the green line highlights the syntenic pair of CCoAOMT genes (*JrCCoAOMT5* and *JrCCoAOMT10)*. (B) Interspecific synteny analysis of CCoAOMT genes between walnut and three other plant species. From top to bottom: walnut vs. *Juglans nigra*(Jn), walnut vs. *Carya cathayensis*(Cc), and walnut vs. *Arabidopsis thaliana* (At). Orange bars represent walnut chromosomes, green bars represent chromosomes of the corresponding species, and red lines indicate homologous CCoAOMT gene pairs between species.

3.5 Functional validation of the walnut *JrCCoAOMT3* gene

Through genome-wide identification, phylogenetic analysis, and synteny analysis, we systematically characterized the walnut CCoAOMT gene family at the genome-wide level, clarifying the sequence features, evolutionary relationships, and genomic distribution of family

members. Among them, *JrCCoAOMT3* not only shares high sequence conservation with functionally characterized CCoAOMT orthologs from Arabidopsis thaliana and other land plants, suggesting it may retain the core function of regulating phenylpropanoid metabolism and secondary cell wall synthesis, but also arises from a segmental duplication event with *JrCCoAOMT2* within the walnut genome, giving it species-specific functional divergence potential. Thus, *JrCCoAOMT3* is the most valuable core member of the walnut CCoAOMT family for further study. Transcriptome data from different developmental stages of walnut endocarp showed that the expression level of *JrCCoAOMT3* was significantly higher than that of other members, and its expression pattern closely matched the lignification process of the endocarp. This expression characteristic suggests that *JrCCoAOMT3* may play a dominant role in lignin synthesis in walnut endocarp. Therefore, this study selected *JrCCoAOMT3* as the candidate gene for further validation experiments.

3.6 Spatiotemporal expression analysis of *JrCCoAOMT3*

RNA was extracted from different tissues and different developmental stages of walnut, and reverse transcription products obtained by the one-step method were used for real-time quantitative PCR. The relative expression of the *JrCCoAOMT3* gene in different walnut tissues is shown in Figure 5A. Using expression in vegetative branches as the control, *JrCCoAOMT3* expression was highest in flowers, being significantly upregulated by 315.95%; it was also significantly upregulated in fruiting branches and leaves by 326.79% and 198.49%, respectively. In contrast, expression was significantly downregulated in endocarp (non-hardened), endocarp (hardened), kernel, endopleura, and exocarp, with the most pronounced downregulation in hardened endocarp and kernel, by 97.56% and 99.45%, respectively. The relative expression of *JrCCoAOMT3* during all developmental stages of walnut is shown in Figure 5B, using the PA stage as the control. The results showed that *JrCCoAOMT3* expression sharply increased at the PD stage and reached the highest level at the PE stage, approximately 6.40-fold and 8.02-fold higher than the control, respectively, both significantly higher than in other stages ($P < 0.05$). Expression dropped sharply at the SB stage, rose slightly at the SC stage, fell again at the SD stage, then increased slightly at the SE stage, but remained below the control level overall. Expression

increased slightly at the SF stage and then remained low during the PA, PB, and PC stages. These results indicate that *JrCCoAOMT3* may play a key regulatory role during the PD and PE stages of walnut growth and development.

3.7 Cloning and subcellular localization of *JrCCoAOMT3*

To analyze the subcellular localization of *JrCCoAOMT3*, the *JrCCoAOMT3* coding sequence was fused with GFP to construct a 35S::*JrCCoAOMT3*-GFP fusion protein expression vector. The construct was transiently expressed in tobacco leaves, and fluorescence was observed by confocal laser scanning microscopy. As shown in Figure 5C, green fluorescence was observed in both the cytoplasm and the nucleus of tobacco leaf cells infiltrated with GFP alone. Co-localization of green and red fluorescence showed that the *JrCCoAOMT3*-GFP fluorescence signal was concentrated in a few cytoplasmic regions, where the merged signal appeared yellow. Therefore, *JrCCoAOMT3* was determined to be a cytoplasmic protein, indicating that it functions in the cytoplasm.

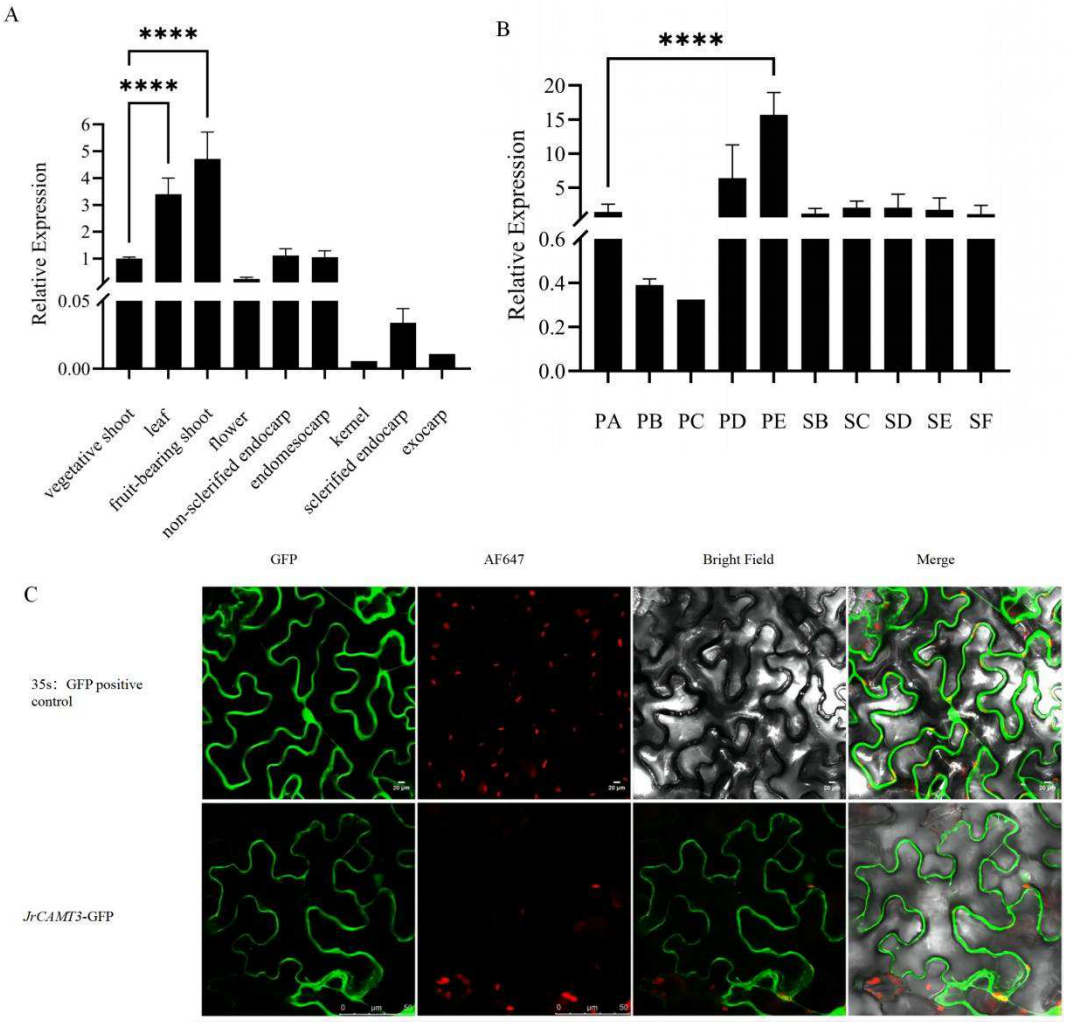


Fig. 5 Expression patterns of *JrCCoAOMT3* gene and subcellular localization of *JrCCoAOMT3* protein. (A) Relative expression levels of *JrCCoAOMT3* in different walnut tissues. The expression level in vegetative shoot was set as the calibrator . (B) Relative expression levels of *JrCCoAOMT3* in walnut fruits at ten different developmental stages (PA to SF). (C) Subcellular localization of *JrCCoAOMT3* protein in Nicotiana benthamiana epidermal cells. The 35S:GFP vector was used as a positive control. Green fluorescence indicates GFP signal, red fluorescence indicates chloroplast autofluorescence detected in the AF647 channel. All qRT-PCR assays were performed with three independent biological replicates and three technical replicates. The *Jr18s* gene was used as the internal reference, and relative expression levels were calculated using the 2^-ΔΔCt method. Error bars represent the standard error (SE) of three biological replicates. **** indicates a statistically significant difference at $p < 0.0001$.

3.8 Identification of *JrCCoAOMT3*-overexpressing Arabidopsis thaliana positive plants

Fresh green leaf tissue from *JrCCoAOMT3*-overexpressing Arabidopsis thaliana plants was collected for DNA extraction. Detection of the T-DNA sequence of Agrobacterium GV3101 in the plant DNA served as the basic criterion for confirming transgenic plants. The target sequence

length was 448 bp. PCR identification was performed using DNA from healthy green leaf tissue of wild-type Arabidopsis thaliana plants as a negative control. As shown in Fig. 6-D, all 16 transgenic plants exhibited clear hygromycin resistance and were identified as overexpressing transgenic plants. The expression level of *JrCCoAOMT3* in each line was further examined by qRT-PCR, and based on the results, lines *JrCCoAOMT3*-OE1, *JrCCoAOMT3*-OE7, and *JrCCoAOMT3*-OE8, which showed high expression, were selected for subsequent experiments.

3.9 Observation and analysis of *JrCCoAOMT3*-overexpressing Arabidopsis thaliana plants

The phenotype of *JrCCoAOMT3*-overexpressing A. thaliana plants was compared with that of wild-type plants. As shown in Figure 6A, the overexpressing plants exhibited more vigorous growth, although the difference in stem diameter was not obvious. Further measurements of stem diameter and plant height during growth revealed results consistent with the visual observations: the average stem diameter of *JrCCoAOMT3*-overexpressing plants was approximately 0.86 mm, slightly less than that of the wild-type, but the difference was not significant (Figure 6B). However, plant height was significantly increased in *JrCCoAOMT3*-overexpressing plants, reaching approximately 36.06 cm, which was about 7.26 cm higher than the control group (Figure 6C).

Observation of differences in stems and siliques between wild-type and *JrCCoAOMT3*-overexpressing plants (Figure 6G) showed that the stem diameter of overexpressing plants was slightly reduced, but the difference was not significant, while the silique volume was significantly reduced. Quantitative analysis of silique length, silique diameter, and silique weight during A. thaliana growth revealed that average silique length and diameter of *JrCCoAOMT3*-overexpressing plants were not significantly different from those of the wild-type (Figure 6E, F). However, the average silique weight of overexpressing plants was significantly reduced by 26.47% compared to the wild-type, being only 0.25 g (Figure 6H).

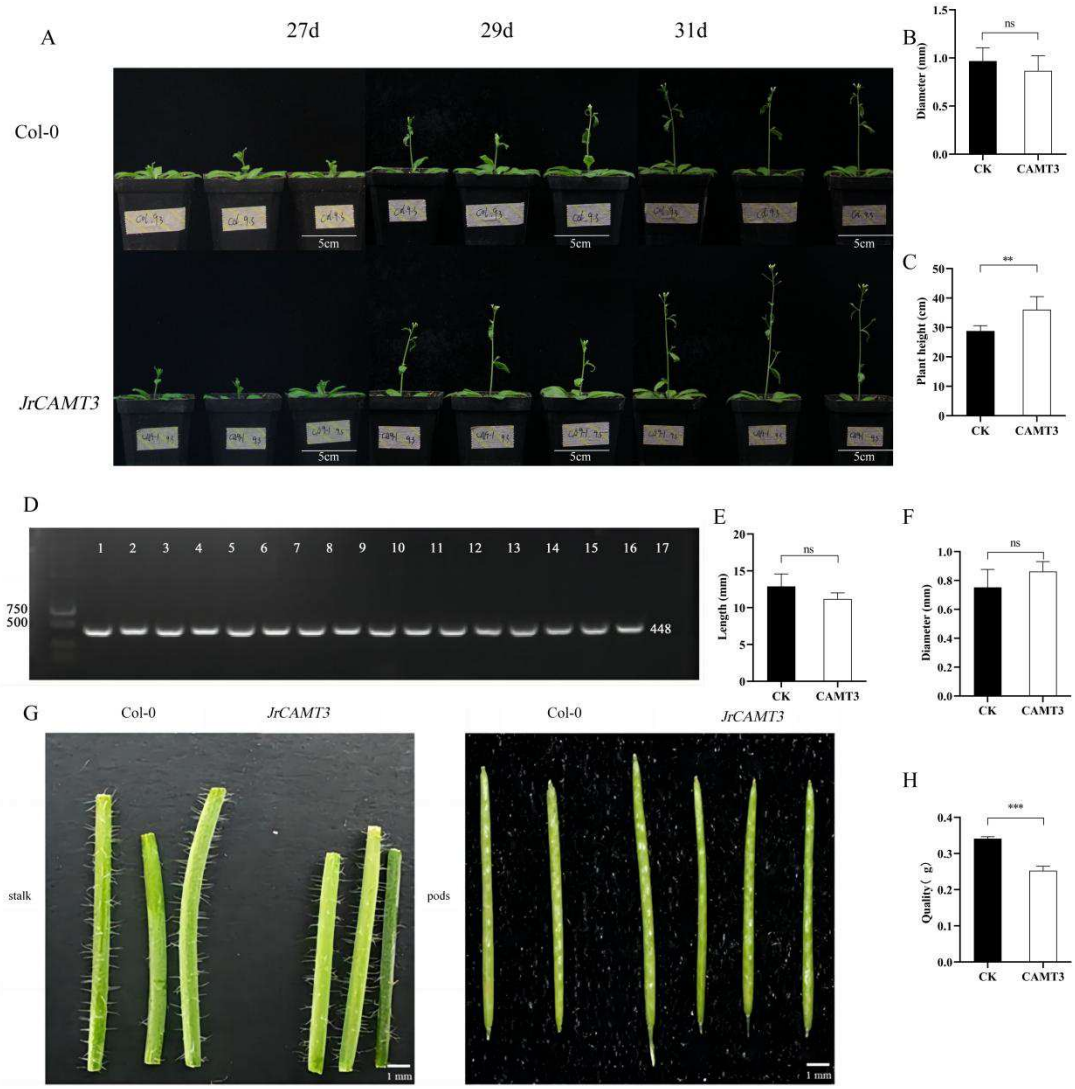


Fig. 6 Phenotypic analysis of *JrCCoAOMT3*-overexpressing Arabidopsis thaliana plants.

(A)Growth phenotypes of wild-type (col) and *JrCCoAOMT3*-overexpressing Arabidopsis plants at 27, 29 and 31 days after sowing. Scale bar = 5 cm.(B) Stem diameter of wild-type and *JrCCoAOMT3*-overexpressing plants.(C) Plant height of wild-type and *JrCCoAOMT3*-overexpressing plants.(D) PCR identification of *JrCCoAOMT3*-overexpressing positive lines. Lanes 1-16: 16 positive transgenic lines; lane 17: negative control. The target fragment size is 448 bp.(E) Silique length of wild-type and *JrCCoAOMT3*-overexpressing plants.(F) Silique diameter of wild-type and *JrCCoAOMT3*-overexpressing plants.(G) Morphological observation of stems and siliques from wild-type and *JrCCoAOMT3*-overexpressing plants. Scale bar = 1 mm.(H) Silique weight of wild-type and *JrCCoAOMT3*-overexpressing plants.All data are presented as mean ± standard deviation (SD) of three biological replicates. ns indicates no significant difference; ** indicates $p < 0.01$; *** indicates $p < 0.001$.

3.10 Spatiotemporal expression analysis of *JrCCoAOMT3* in overexpressing Arabidopsis thaliana

Using wild-type Arabidopsis thaliana as the control and GAPDH as the reference gene, the expression levels of *JrCCoAOMT3* in roots, stems, leaves, flowers, and siliques of

JrCCoAOMT3-overexpressing Arabidopsis plants were analyzed. As shown in Fig. 7-B, the relative expression of *JrCCoAOMT3* was significantly higher in all tested tissues of overexpressing plants compared to the wild-type, with the highest expression observed in stems and siliques, while the upregulation in roots, leaves, and flowers was relatively smaller.

3.11 Observation of lignified microstructure in different tissues of *JrCCoAOMT3*-overexpressing Arabidopsis thaliana

Toluidine blue staining was used to investigate microstructural changes in stem cross-sections of *JrCCoAOMT3*-overexpressing A. thaliana. As shown in Figure 7A, compared to wild-type stem cross-sections, the gap between the epidermis and cortex in stems of overexpressing plants showed little change, but the number of sclereids in the phloem increased significantly and was more densely packed, and the proportion of intercellular space in the pith also increased markedly.

Observation of silique cross-sections (Figure 7C) showed that, compared to wild-type, the ovary structure of overexpressing plants was enlarged, while the thickness of the ovary wall did not change significantly. However, the cells of the ovary wall were arranged more densely, the ovules were more uniform and plump, but the placenta in the central region of the ovary was lost.

Further quantitative analysis of the microstructures of siliques and stems using ImageJ showed that, compared to wild-type, the longitudinal diameter of the stem cross-section in *JrCCoAOMT3*-overexpressing plants was 1680.00 μm, an increase of 23.77%; the transverse diameter was 705.33 μm, with no significant difference compared to wild-type (Figure 7D). Regarding siliques, the longitudinal diameter of the silique cross-section in overexpressing plants was 1154.67 μm, a significant increase of 16.55% compared to wild-type; the transverse diameter was 904.00 μm, a significant increase of 6.44% (Figure 7E).

Lignified regions in stem cross-sections of wild-type and *JrCCoAOMT3*-overexpressing plants were stained to explore the effect of *JrCCoAOMT3* on the proportion of lignified area relative to the total stem cross-sectional area. The results are shown in Figure 7G.

Scanning electron microscopy was used to observe the effect of *JrCCoAOMT3* overexpression on stem cell wall thickness in A. thaliana. As shown in Figure 7F, compared to

wild-type, the plasma membrane of stem cells in *JrCCoAOMT3*-overexpressing plants exhibited peeling, the middle lamella was thickened, and the secondary wall, which forms between the plasma membrane and the middle lamella, was reduced in thickness, with unclear morphological structure; the intact cell wall thickness was reduced. Quantitative analysis of cell wall thickness using ImageJ indicated that, compared to wild-type, the overall stem cell wall thickness in *JrCCoAOMT3*-overexpressing plants decreased, but the difference was not significant (Figure 7I, right). It is speculated that *JrCCoAOMT3* may be involved in the synthesis of substances in the cell wall, thereby causing changes in cell wall thickness and morphology.

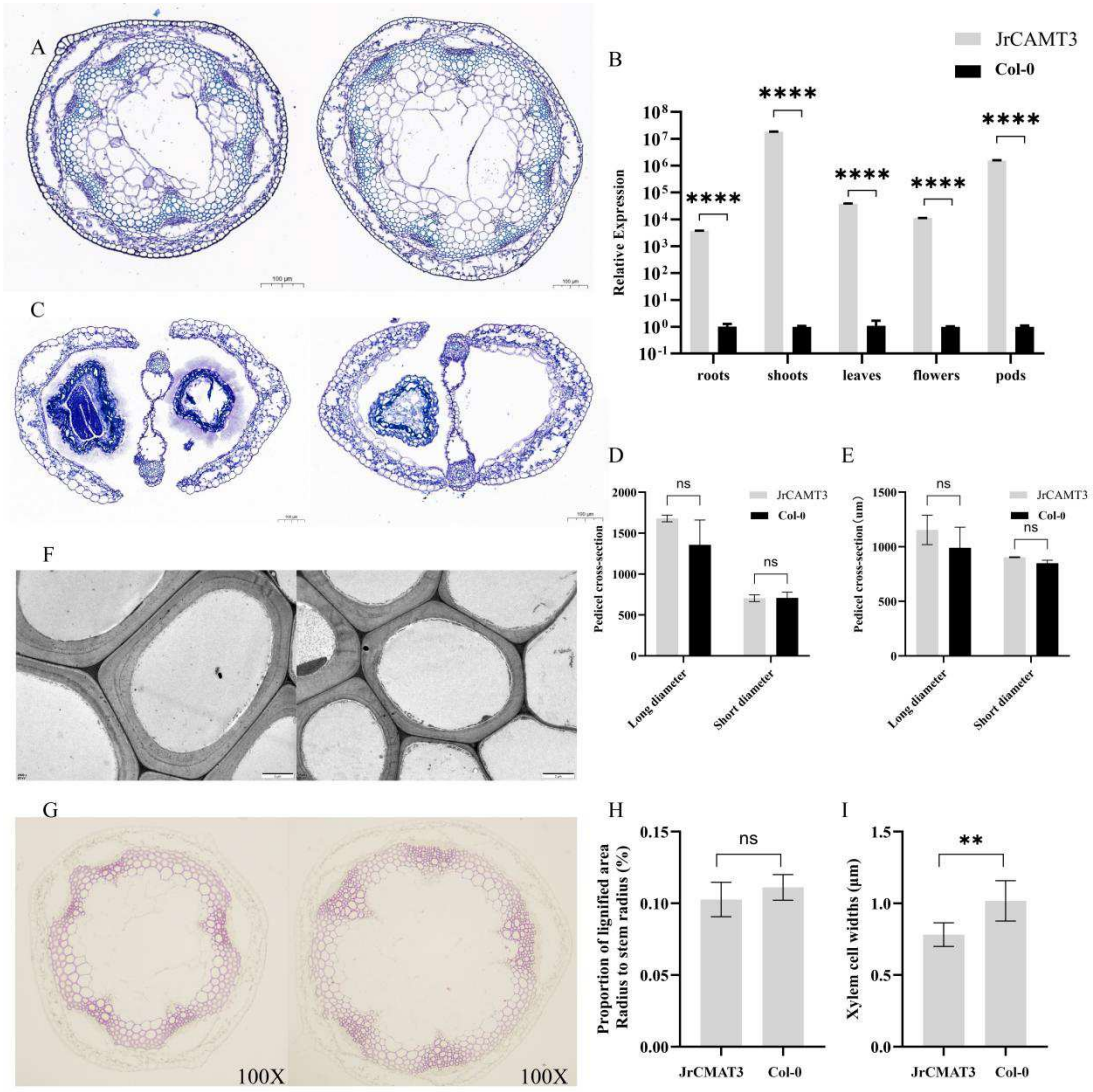


Fig. 7 Histological observation and quantitative analysis of *JrCCoAOMT3*-overexpressing A. thaliana plants. (A) Toluidine blue staining of stem cross-sections from wild-type (Col-0) and *JrCCoAOMT3*-overexpressing plants. Scale bar = 100 μm. (B) Relative expression levels of *JrCCoAOMT3* in different tissues of wild-type and overexpressing plants. (C) Toluidine blue staining of silique pedicel

cross-sections from wild-type and *JrCCoAOMT3*-overexpressing plants. Scale bar = 100 μm. (D) Quantitative analysis of stem cross-section long and short diameters in wild-type and overexpressing plants. (E) Quantitative analysis of silique pedicel cross-section long and short diameters in wild-type and overexpressing plants. (F) Scanning electron microscopy observation of xylem cell walls in stems of wild-type and *JrCCoAOMT3*-overexpressing plants. Scale bar = 1 μm. (G) Phloroglucinol-HCl staining of lignified regions in stem cross-sections of wild-type and *JrCCoAOMT3*-overexpressing plants. Magnification: 100×. (H) Ratio of lignified region radius to total stem radius in wild-type and overexpressing plants. (I) Quantitative analysis of xylem cell wall thickness in stems of wild-type and overexpressing plants. All data are presented as mean ± standard deviation (SD) of three biological replicates. ns indicates no significant difference; ** indicates $p < 0.01$; **** indicates $p < 0.0001$.

3.12 Determination of lignin content in different tissues of *JrCCoAOMT3*-overexpressing Arabidopsis thaliana

Samples were extracted from leaves, roots, siliques, and stems of wild-type and *JrCCoAOMT3*-overexpressing A. thaliana plants, and the contents of hemicellulose, cellulose, and total lignin were measured. The results showed that, compared to wild-type, hemicellulose content in leaves of overexpressing plants slightly decreased, while that in roots significantly increased by 27.29%; hemicellulose content in stems and siliques also significantly increased by 35.72% and 58.79%, respectively (Figure 8A). Cellulose content was significantly higher in all tissues of overexpressing plants than in wild-type, with increases of 33.41% in leaves, 29.57% in roots, 217.62% in siliques, and 36.86% in stems (Figure 8B). Regarding lignin content, siliques and stems of overexpressing plants showed significant increases of 134.30% and 45.64%, respectively, compared to wild-type, while lignin content in roots increased slightly but not significantly (Figure 8C).

Leaves, siliques, and stem bases were collected from overexpressing (*JrCCoAOMT3*-OE1, OE7, OE8) and wild-type A. thaliana plants. The contents of G-type, H-type, and S-type lignin monomers were determined by high-performance liquid chromatography (HPLC). The results showed that, compared to wild-type, the H-type lignin content in leaves of overexpressing lines was significantly reduced by 26.5%, and in siliques by 40.0%; in stems, G-type lignin content was

significantly increased by 19.6%, while H-type content was significantly reduced by 29.5%, and S-type content showed no significant change (Figure 8D-F). These results indicate that overexpression of *JrCCoAOMT3* significantly inhibits the accumulation of lignin monomers in leaves and siliques but specifically promotes the synthesis of G-type lignin in stems. This finding is consistent with the observed significant increase in total lignin content and changes in cell wall structure in stems, further confirming the tissue-specific regulatory role of *JrCCoAOMT3* in lignin metabolism.

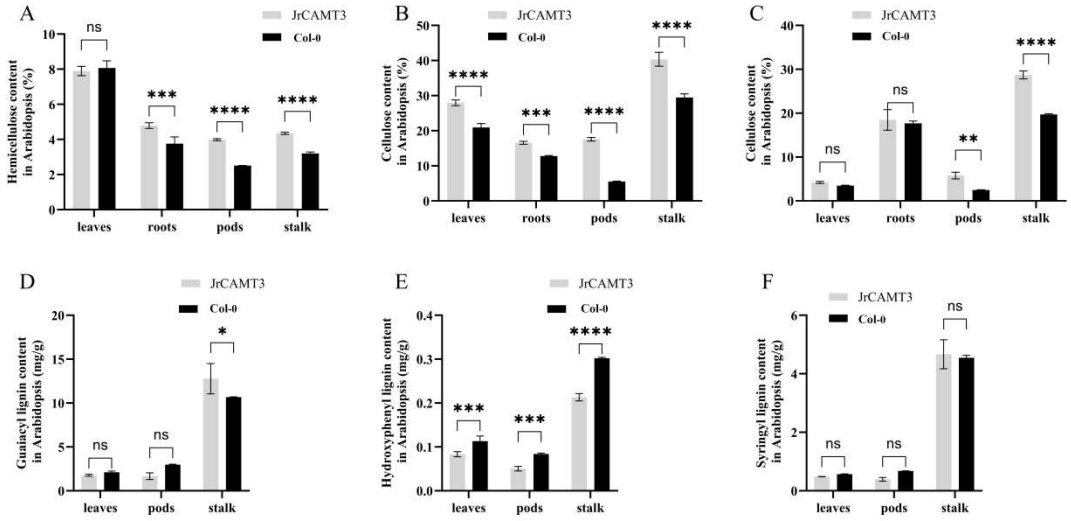


Figure 8. Contents of hemicellulose, cellulose, lignin and lignin monomers in different tissues of *JrCCoAOMT3*-overexpressing A. thaliana plants.

(A) Hemicellulose content in leaves, roots, pods and stalks of wild-type (Col-0) and *JrCCoAOMT3*-overexpressing plants. (B) Cellulose content in leaves, roots, pods and stalks of wild-type and *JrCCoAOMT3*-overexpressing plants. (C) Lignin content in leaves, roots, pods and stalks of wild-type and *JrCCoAOMT3*-overexpressing plants. (D) Guaiacyl lignin content in leaves, pods and stalks of wild-type and *JrCCoAOMT3*-overexpressing plants. (E) Hydroxyphenyl lignin content in leaves, pods and stalks of wild-type and *JrCCoAOMT3*-overexpressing plants. (F) Syringyl lignin content in leaves, pods and stalks of wild-type and *JrCCoAOMT3*-overexpressing plants. All data are presented as mean ± standard deviation (SD) of three biological replicates. ns indicates no significant difference; * indicates $p < 0.05$; ** indicates $p < 0.01$; *** indicates $p < 0.001$; **** indicates $p < 0.0001$.

4. DISCUSSION

Lignin is a complex aromatic polymer and a major component of the plant cell wall, which provides structural support and protection for plants against environmental stresses such as wind, rain, and pest infestation [7]. In walnut, lignin is mainly deposited in the outer layers of the nut, including the exocarp and endocarp[32].

Lignin affects the taste and aroma of walnut kernels. As walnuts age, lignin in the kernel cell walls degrades, releasing compounds that contribute to the formation of a bitter and astringent taste [16]. This effect is particularly pronounced in walnuts stored improperly or for an excessively long period [29]. In terms of flavor and aroma, studies have found that the concentrations of lignin-derived compounds such as vanillin and syringaldehyde increase during walnut storage, resulting in enhanced bitterness and stronger aroma [29]. Meanwhile, higher concentrations of certain lignin-derived compounds have been detected in aged walnuts, which leads to intensified astringency [16].

In addition, lignin biosynthesis in walnut has been confirmed to be associated with various biological processes, including fruit development [13][5][39][60], abiotic stress resistance [4][51][62][8][70][61][9], and disease resistance [45][15][67][38][41][34][55][58][19][66]. Previous studies have elucidated the molecular mechanism of lignin biosynthesis in walnut trees under drought stress, and identified genes involved in the lignin biosynthetic pathway that were upregulated in response to drought stress [63]. Furthermore, infection by the fungus Botryosphaeria dothidea was found to cause upregulation of several genes involved in the lignin biosynthetic pathway, indicating that lignin may play a role in walnut defense against fungal pathogens [26].

The primary effect of lignin on walnut quality is reflected in its influence on the mechanical properties of the nut. Lignin also plays a critical role in maintaining the structural integrity of the nut and preventing damage during growth and harvesting. Several studies have investigated the effects of lignin on walnut quality. For example, increased lignin content in walnut shells leads to enhanced mechanical strength but reduced kernel yield, and lignin content shows a negative correlation with nut yield and cracking efficiency [16]. Numerous scholars have explored the relationship between walnut shell structure (suture tightness, thickness, mechanical strength) and

559 the commercial quality of kernels [46][56][42][69]. It has been found that thicker walnut shells are
560 accompanied by tighter sutures; shell thickness shows an extremely significant positive correlation
561 with nut weight and an extremely significant negative correlation with kernel yield [71][2]. However,
562 the presence of lignin in the shell also increases the difficulty of extracting edible kernels, as
563 lignin-rich shells are hard and resistant to cracking [1].

564 The CCoAOMT gene is one of the key genes in the lignin biosynthesis pathway. To further
565 explore the relationship between this gene and endocarp lignification in walnut, we performed
566 bioinformatics analysis including gene structure, conserved motifs, interspecific collinearity, and
567 cis-acting element prediction to reveal the potential biological functions of these genes. In this
568 study, a total of 11 JrCCoAOMT family genes were identified in walnut. This number is
569 substantially different from that in Isatis indigotica [30], Camellia sinensis [53], and Platycodon
570 grandiflorus [36], in which 8, 10, and 5 CCoAOMT members were identified, respectively.

571 Analysis of the structural characteristics of JrCCoAOMT genes led to the identification of 10
572 conserved motifs. The results showed that all JrCAMT proteins contained Motif 1 and Motif 3,
573 which is consistent with the findings on CCoAOMT in Capsicum annuum [28]. Members within
574 the same subfamily shared similar motif composition patterns, which is in agreement with the
575 research conclusions in Setaria italica [23]. It is speculated that the functions of JrCCoAOMT
576 genes in plant growth and development are highly conserved.

577 Physicochemical property analysis revealed that most members of the walnut JrCCoAOMT
578 family are hydrophilic proteins. The high hydrophilicity of these proteins can enhance their
579 solubility and stability in the aqueous cytoplasmic environment [18]. Among them, 91% of the
580 proteins were acidic, suggesting that they may function in acidic subcellular environments, which
581 is consistent with the research of Wang et al.[54].

582 Predictive analysis of cis-acting elements in the promoter region of JrCCoAOMT genes
583 showed the ubiquitous presence of light-responsive elements, implying that the expression of
584 JrCAMT family genes may be light-dependent. This is similar to previous studies reporting that
585 lignin biosynthesis is regulated by light signals [52]. In addition, a large number of cis-elements
586 related to hormone response and stress tolerance were also identified.

587 Lignin, polymerized from H-, G-, and S-type monolignols, is a major component of plant
588 secondary cell walls and critically determines the mechanical properties of woody tissues

including walnut endocarp [3][32]. Within the phenylpropanoid pathway, CCoAOMT canonically catalyzes the methylation of caffeoyl-CoA to feruloyl-CoA, thereby supplying precursors for G- and S-type but not H-type lignin, which derives from the non-methylated p-coumaroyl-CoA [72][21]. In this study, genome-wide identification recovered 11 JrCCoAOMT members in walnut, among which *JrCCoAOMT3* exhibited peak expression at the PD/PE stages (78–92 DAFB) coincident with active endocarp lignification [30], and cytoplasmic localization consistent with the enzyme's metabolic context. Heterologous overexpression in Arabidopsis revealed a distinctive lignin monomer shift: H-type lignin was significantly reduced across leaves, siliques and stems, while G-type lignin was specifically increased in stems, with S-type unchanged. This tissue-biased monomer reallocation — H↓ globally, G↑ restricted to stems — is noteworthy because it diverges from the more commonly reported CCoAOMT overexpression phenotypes in herbaceous models, where total lignin typically decreases [43] or S-type increases [57]. Two non-mutually exclusive mechanisms may account for the H↓ effect: (i) competitive diversion of the shared precursor p-coumaroyl-CoA into the methylation flux, depleting the H-unit precursor pool [49]; and (ii) feedback or functional redundancy with COMT, as suggested by CCoAOMT–COMT interplay in alfalfa [22]. The stem-restricted G↑ further raises the possibility that *JrCCoAOMT3* exhibits tissue-specific substrate preference or interacts with stem-specific cofactors, analogous to *GhCCoAOMT7* in cotton fibers[35] . We therefore interpret *JrCCoAOMT3* not as a H-type-specific regulator, but as a modulator of lignin monomer allocation with tissue-dependent outputs — a nuance that may be general to CCoAOMT isoforms in woody crops and worth testing via in vitro enzyme kinetics in future work.

Lignin is the main component of the secondary cell wall, and its significant increase in stems can improve the mechanical strength, stress resistance, and disease resistance of plants. *JrCCoAOMT3* is involved in the phenylpropanoid pathway of lignin biosynthesis in A. thaliana siliques. Its overexpression increased the content of cafestol, and most phenylpropanoids such as phenylpropionic acid and coumaraldehyde were elevated in stems. However, the stem volume of A. thaliana was reduced while the major and minor diameters of the stem cross-section were significantly increased, which is attributed to the densification of the secondary cell wall, indicating that cells were elongated and expanded rather than hyperplastic.

618 The significant reduction in silique volume accompanied by an increase in the major
619 diameter of the silique cross-section is due to the enhanced cell wall extensibility and
620 expandability caused by the increased hemicellulose content in siliques. In addition,
621 overexpression of *JrCCoAOMT3* also led to a significant decrease in H-type lignin content in A.
622 thaliana, while it had no significant effect on the biosynthesis of S-type and G-type lignin, and
623 significantly increased G-type lignin content in stems.
624 This result is different from previous studies. For example, overexpression of the CCoAOMT
625 gene in switchgrass resulted in reduced lignin content and increased S-type lignin monomer
626 content, which was associated with improved biomass digestibility [57]. Similarly, downregulation
627 of the CCoAOMT gene in poplar caused reduced lignin content and altered cell wall composition,
628 thereby affecting plant growth and development [43]. However, overexpression of the CCoAOMT
629 gene in alfalfa led to increased lignin content and reduced G-type lignin monomer content, which
630 was related to improved digestibility [22].
631 The ratio of S-type to G-type lignin units is a key chemical property that determines the
632 physicochemical characteristics of lignin. It has been well documented that the S/G ratio directly
633 affects the mechanical properties of plant secondary cell walls: an elevated S/G ratio generally
634 confers higher hardness and brittleness to the cell wall, whereas a reduced S/G ratio leads to
635 enhanced flexibility and elasticity of cell wall structures [50][6]. This compositional variation further
636 modulates the adaptability of plants to external mechanical stresses such as wind load and gravity.
637 CCoAOMT catalyzes the methylation of caffeoyl-CoA to feruloyl-CoA, a precursor for G-
638 and S-type lignin units. However, our observation that *JrCCoAOMT3* overexpression drastically
639 reduces H-type lignin while only increasing G-lignin in stems is intriguing and deserves
640 mechanistic explanation. Given that H-type lignin is derived from non-methylated p-coumaryl
641 alcohol, the reduction in H-lignin could be a consequence of increased flux through the
642 methylation pathway, depleting the pool of p-coumaroyl-CoA (the direct precursor for H-unit
643 formation). This competitive substrate consumption mechanism has been proposed in other
644 systems where CCoAOMT overexpression altered the S/G/H composition [49]. Alternatively, the
645 tissue-specific effect on G-lignin in stems might reflect differential promoter activity or the
646 presence of tissue-specific cofactors that modulate *JrCCoAOMT3* substrate specificity. In cotton,
647 GhCCoAOMT7 was shown to preferentially affect G-lignin in fibers, indicating that CCoAOMT

isoforms can have different in vivo substrate preferences [35]. Thus, *JrCCoAOMT3* may have evolved a distinct substrate preference or interaction partner that directs its activity toward G-unit production specifically in lignified stem tissues. Future enzyme kinetic studies and metabolic flux analyses are needed to test these hypotheses.

In our study, *JrCCoAOMT3* expression peaked at the PD (78 days after full bloom) and PE (92 days after full bloom) stages, which coincide with the active lignification period of walnut endocarp (70–100 DAFB), as confirmed by anatomical observations of stone cell deposition and lignin accumulation in 'Xinlu' walnut [27][31]. The observed downregulation of *JrCCoAOMT3* in hardened endocarp compared to non-hardened endocarp is consistent with the typical transient expression pattern of secondary wall biosynthesis genes, which are highly expressed during the initiation and early deposition phases but decline after wall thickening is complete. This temporal pattern further supports the role of *JrCCoAOMT3* in the active phase of lignification rather than in maintenance of lignin content in mature tissues.

Recent multi-omics studies have identified a suite of genes associated with walnut endocarp development, including *CCoAOMT1, CCoAOMT7, MYB308, MYB83, NAC043* and *NAC073*, which are co-expressed during lignification [30]. Heterologous expression of walnut *JrUGP* and *JrMYB308* in A. thaliana confirmed their roles in lignin biosynthesis and secondary wall thickening [33]. Our study adds *JrCCoAOMT3* to this regulatory network and provides evidence for its role in modulating lignin monomer composition. Moreover, a transcriptomic analysis by Li et al. [27] revealed that *JrMYB180* is significantly induced by GA_3 treatment and likely acts upstream of lignin biosynthetic genes in walnut endocarp. It is plausible that *JrCCoAOMT3* is also a target of GA_3-mediated regulation, given the temporal overlap of its expression peak with GA_3-responsive stages. Further investigation of the transcriptional regulation of *JrCCoAOMT3* by *MYB* and *NAC* transcription factors will be valuable for understanding the hierarchical control of walnut shell lignification.

We acknowledge that all functional validation in this study was performed in A. thaliana due to the lack of a stable transformation system for walnut. This limitation is common in woody plant research and does not diminish the significance of our findings, as many walnut lignin-related genes have been successfully characterized via heterologous expression [28][33]. Nevertheless, direct functional studies in walnut—such as transient overexpression, RNA

interference, or virus-induced gene silencing (VIGS) in developing fruits—are urgently needed to confirm the in vivo role of *JrCCoAOMT3* in endocarp lignification. Additionally, in vitro enzyme activity assays and substrate specificity tests would clarify whether *JrCCoAOMT3* preferentially methylates caffeoyl-CoA or acts on other phenylpropanoid intermediates, which would help explain its distinct effect on H-type lignin. Metabolomic profiling of transgenic walnut tissues would further reveal the flux changes in lignin biosynthetic pathways.

5. CONCLUSION

In this study, a total of 11 JrCCoAOMT gene family members were genome-wide identified in walnut (Juglans regia L.), and their sequence characteristics, gene structure, chromosomal distribution, and evolutionary patterns were systematically analyzed. The results showed that these 11 JrCCoAOMT genes were unevenly distributed on 5 chromosomes of the walnut genome. Phylogenetic analysis divided the 45 CCoAOMT members from six related species into 8 subfamilies (Group I–VIII), and JrCCoAOMT genes within the same subclade shared highly conserved gene structure and conserved motif composition, indicating their functional conservation during plant evolution. Collinearity analysis further revealed that both tandem duplication and segmental duplication events drove the expansion of the walnut CCoAOMT gene family, with 2 tandem duplication events and 4 segmental duplication gene pairs identified.

In-depth functional characterization of *JrCCoAOMT3*, the core member of the family, showed that the gene exhibited a specific spatiotemporal expression pattern during walnut fruit development. Its expression level peaked at the PD and PE stages, highly consistent with the lignification process of walnut endocarp, while extremely low expression levels were detected in walnut kernels, middle endocarp, and exocarp. Subcellular localization analysis confirmed that the *JrCCoAOMT3* protein is localized in the cytoplasm.

Heterologous overexpression of *JrCCoAOMT3* in A. thaliana resulted in altered stem and silique morphology, increased hemicellulose and total lignin content, and a specific reduction in H-type lignin across tissues while increasing G-lignin only in stems. These results confirm that *JrCCoAOMT3* plays a key regulatory role in plant cell wall component accumulation, particularly in modulating lignin monomer composition. The study provides a solid theoretical foundation for

706 further understanding of walnut endocarp lignification and offers candidate gene resources for
707 breeding walnut varieties with improved shell traits.

708 **Declarations**

709 **Abbreviations**

710 CCoAOMT: Caffeoyl-CoA O-methyltransferase; DAFB: Days after full bloom; GC-MS: Gas
711 chromatography-mass spectrometry; HPLC: High-performance liquid chromatography; qRT-PCR:
712 Quantitative real-time PCR; SEM: Scanning electron microscopy; VIGS: Virus-induced gene
713 silencing.

714 **Ethics approval and consent to participate**

715 Not applicable.

716 **Consent for publication**

717 Not applicable.

718 **Availability of data and materials**

719 The datasets generated and/or analysed during the current study are available from the
720 corresponding author on reasonable request.

721 **Competing interests**

722 The authors declare that they have no known competing financial interests or personal
723 relationships that could have appeared to influence the work reported in this paper.

724 **Funding**

725 This work was supported by the Special Project for Innovation and Development of Key
726 Industries in Southern Xinjiang of XPCC (Grant No. 2022DB022), the Tianshan Talent Training

Program (Grant No. 2022TSYCCX0120), the National Natural Science Foundation of China (Grant Nos. 31260469, 32160698), the President's Fund of Tarim University (Grant No. TDZKBS202419), the Guiding Science and Technology Plan Project of XPCC (Grant No. 2024ZD113), and the XPCC Youth Science Foundation Project (Grant No. 2026DB028).

Authors' contributions

Ruixia Gao: Visualization, Formal analysis, Data curation; Shangqi Yu: Resources, Writing – review & editing; Yonglin Shao: Writing – original draft, Visualization, Data curation; Qian Ye: Writing – review & editing; Xingyu Guo: Writing – review & editing; Qiang Jin: Writing – review & editing, Supervision; Rui Zhang: Writing – review & editing, Project administration, Methodology; Zhongzhong Guo: Writing – review & editing, Funding acquisition, Data curation. All authors read and approved the final manuscript.

Acknowledgements

The authors sincerely appreciate the financial support from the funding programs listed above.

References

[1] Akça, Y., 2000. Determination of fruit growth and development in walnut. Turkish Journal of Agriculture & Forestry 24, 671-676.

[2] Arzani, K., Mansouri-Ardakan, H., Vezvaei, A., 2008. Morphological variation among Persian walnut (Juglans regia) genotypes from central Iran. New Zealand Journal of Agricultural Research 36, 159-168. https://doi.org/10.1080/01140670809510232

[3] Boerjan, W., Ralph, J., Baucher, M., 2003. Lignin biosynthesis. Annual Review of Plant Biology 54, 519-546. https://doi.org/10.1146/annurev.arplant.54.031902.134938

[4] Cabane, M., Afif, D., Hawkins, S., 2012. Lignins and abiotic stresses. In: Jouann, L., Lapierre, C. (Eds.), Lignins: Biosynthesis, Biodegradation and Bioengineering, Vol. 61. Elsevier Academic Press, San Diego, pp. 219-262. https://doi.org/10.1016/B978-0-12-416023-1.00007-0

[5] Cai, Y., Li, G., Nie, J., Lin, Y., 2010. Study of the structure and biosynthetic pathway of lignin in stone cells of pear. Scientia Horticulturae 125, 374-379. https://doi.org/10.1016/j.scienta.2010.04.029

[6] Cao, Y., Yan, X., Ran, S., Liu, J., Li, J., Fang, X., Wang, Z., 2022. Knockout of the lignin pathway gene BnF5H decreases the S/G lignin compositional ratio and improves Sclerotinia sclerotiorum resistance in Brassica napus. Plant, Cell & Environment 45, 248-261. https://doi.org/10.1111/pce.14208

[7] Chen, F., Dixon, R.A., 2007. Lignin modification improves fermentable sugar yields for biofuel production. Nature Biotechnology 25, 759-761. https://doi.org/10.1038/nbt1316

[8] Chen, X., Li, N., Liu, C., Zhang, Z., Li, C., Ma, F., 2024. Exogenous GABA improves the resistance of apple seedlings to long-term drought stress by enhancing GABA shunt and secondary cell wall biosynthesis. Tree Physiology 44, 345-358. https://doi.org/10.1093/treephys/tpad153

[9] Chen, Y., Yi, N., Yao, S.B., Liu, S.Y., Tang, H., Ruan, J.C., 2021. CsHCT-mediated lignin synthesis pathway involved in the response of tea plants to biotic and abiotic stresses. Journal of Agricultural and Food Chemistry 69, 10069-10081. https://doi.org/10.1021/acs.jafc.1c02771

[10] Chou, K.C., Shen, H.B., 2010. A new method for predicting the subcellular localization of eukaryotic proteins with both single and multiple sites: Euk-mPLoc 2.0. PLoS ONE 5, e9931.

[11] Cramer, G.R., Urano, K., Delrot, S., Pezzotti, M., Shinozaki, K., 2011. Effects of abiotic stress on plants: a systems biology perspective. BMC Plant Biology 11, 163. https://doi.org/10.1186/1471-2229-11-163

[12] Do, C.T., Pollet, B., Thévenin, J., Sibout, R., Denoue, D., Barrière, Y., Lapierre, C., Jouanin, L., 2007. Both caffeoyl Coenzyme A 3-O-methyltransferase 1 and caffeic acid O-methyltransferase 1 are involved in redundant functions for lignin, flavonoids and sinapoyl malate biosynthesis in Arabidopsis. Planta 226, 1117-1129. https://doi.org/10.1007/s00425-007-0558-3

[13] Estrada, B., Bernal, M.A., Diaz, J., Pomar, F., Merino, F., 2000. Fruit development in Capsicum annuum: changes in capsaicin, lignin, free phenolics, and peroxidase patterns.

782 Journal of Agricultural and Food Chemistry 48, 6234-6239.
783 https://doi.org/10.1021/jf000190x
784 [14] Fellenberg, C., Milkowski, C., Hause, B., Lange, P.R., Matern, U., Vogt, T., 2008.
785 Tapetum-specific location of a cation-dependent O-methyltransferase in Arabidopsis
786 thaliana. The Plant Journal 56, 132-145. https://doi.org/10.1111/j.1365-313X.2008.03576.x
787 [15] Fonguimgo, T.F., Hanafi, M.M., Idris, A.S., Sariah, M., Akmar, A.N., 2015. Comparative
788 study of lignin in roots of different oil palm progenies in relation to Ganoderma basal
789 stem rot disease. Journal of Oil Palm Research 27, 128-134.
790 [16] Franklin, L.M., Mitchell, A.E., 2019. Review of the sensory and chemical characteristics of
791 almond (Prunus dulcis) flavor. Journal of Agricultural and Food Chemistry 67, 2743-2753.
792 https://doi.org/10.1021/acs.jafc.8b06606
793 [17] Goujon, T., Sibout, R., Eudes, A., MacKay, J., Jouanin, L., 2003. Genes involved in the
794 biosynthesis of lignin precursors in Arabidopsis thaliana. Plant Physiology and
795 Biochemistry 41, 677-687. https://doi.org/10.1016/S0981-9428(03)00095-0
796 [18] Guo, Z.W., Si, X.Y., Jiao, L.P., Lin, W.X., 2023. Cloning and structural analysis of
797 caffeoyl-CoA O-methyltransferase (CCoAOMT) gene in soybean. Fujian Journal of
798 Agricultural Sciences 38, 616-623.
799 [19] Hoech, K., Koopmann, B., von Tiedemann, A., 2021. Lignin composition and timing of cell
800 wall lignification are involved in Brassica napus resistance to stem rot caused by
801 Sclerotinia sclerotiorum. Phytopathology 111, 1438-1448.
802 https://doi.org/10.1094/PHYTO-09-20-0421-R
803 [20] Hu, B., Jin, J., Guo, A.Y., Zhang, H., Luo, J., Gao, G., 2015. GSDS 2.0: an upgraded gene
804 feature visualization server. Bioinformatics 31, 1296-1297.
805 [21] Humphreys, J.M., Chapple, C., 2002. Rewriting the lignin roadmap. Current Opinion in Plant
806 Biology 5, 224-229. https://doi.org/10.1016/S1369-5266(02)00257-1
807 [22] Inoue, K., Parvathi, K., Dixon, R.A., 2000. Substrate preferences of caffeic
808 acid/5-hydroxyferulic acid 3/5-O-methyltransferases in developing stems of alfalfa
809 (Medicago sativa L.). Archives of Biochemistry and Biophysics 375, 175-182.
810 https://doi.org/10.1006/abbi.1999.1669

811 [23] Jian, P.Y., Zhang, Y.R., Li, X.K., Wang, J., 2026. Identification and expression analysis of
812 SiCCoAOMT gene family in foxtail millet. Acta Prataculturae Sinica 35, 195-209.
813 [24] Lescot, M., Déhais, P., Thijs, G., Marchal, K., Moreau, Y., Van de Peer, Y., Rouzé, P.,
814 Rombauts, S., 2002. PlantCARE, a database of plant cis-acting regulatory elements and a
815 portal to tools for in silico analysis of promoter sequences. Nucleic Acids Research 30,
816 325-327.
817 [25] Li A, Qi S, Zhu Y, Yu H, Wang N, et al. 2026. Ca2+ mediated PbCML46-PbbHLH96 module
818 negatively regulates lignin biosynthesis in pear fruit. Fruit Research 6: e015 doi:
819 10.48130/frures-0026-0011. https://doi.org/10.48130/frures-0026-0011
820 [26] Li, C., Zhang, M., Wei, S., Yang, M., Song, J., Zhang, R., 2023. Study of walnut brown rot
821 caused by Botryosphaeria dothidea in the Guizhou Province of China. Crop Protection
822 163, 106118. https://doi.org/10.1016/j.cropro.2022.106118
823 [27] Li, H., Dai, S., Zhang, W., Liu, Z., Song, Y., Zheng, Y., Xu, M., 2023. Transcriptome analysis
824 of walnut (Juglans regia L.) fruit reveals the function of JrMYB180 in GA_3-induced
825 endocarp lignification. Plant Growth Regulation 100, 647-655.
826 https://doi.org/10.1007/s10725-023-00963-9
827 [28] Li, S., Cai, Y., Ma, H., Wu, Z., Chen, M., 2025. A comprehensive analysis of the
828 O-methyltransferase gene family in the chili pepper (Capsicum annuum) identifies COMT36
829 involved in capsaicinoids biosynthesis. International Journal of Biological Macromolecules
830 312, 144247. https://doi.org/10.1016/j.ijbiomac.2025.144247
831 [29] Liao, M., Zhao, Y., Gong, C., Wang, J., Adhikari, B., 2018. Effects of hot air-assisted radio
832 frequency roasting on quality and antioxidant activity of cashew nut kernels. LWT - Food
833 Science and Technology 93, 274-280. https://doi.org/10.1016/j.lwt.2018.03.047
834 [30] Liu, B., Kong, L., Ma, J., Wang, Z., Li, Q., 2025. Systematic analysis of the CCoAOMT gene
835 family in Isatis indigotica and the molecular mechanism of CCoAOMT8-mediated
836 flavonoid synthesis under alkaline stress treatment. Biology 14, 1518.
837 https://doi.org/10.3390/biology14111518
838 [31] Liu, H., et al., 2025. Integrated multi-omics analyses provide new insights into genomic
839 variation landscape and regulatory network candidate genes associated with walnut endocarp.
840 The Plant Journal 122, e70113. https://doi.org/10.1111/tpj.70113

[32] Liu, Q., Luo, L., Zheng, L., 2018. Lignins: biosynthesis and biological functions in plants. International Journal of Molecular Sciences 19, 335. https://doi.org/10.3390/ijms19020335

[33] Liu, Y.S., Fan, R.Y., Li, Y.D., Chen, H., Li, C.Y., 2025. Evolutionary analysis and bifunctionality of VcCCoAOMT5: a key O-methyltransferase involved in both lignin and anthocyanin biosynthesis in highbush blueberry. Journal of Agricultural and Food Chemistry 73, 7125-7138. https://doi.org/10.1021/acs.jafc.5c08657

[34] Lu, J., Shi, Y., Li, W., Li, H., Liu, A., 2019. RcPAL, a key gene in lignin biosynthesis in Ricinus communis L. BMC Plant Biology 19, 181. https://doi.org/10.1186/s12870-019-1777-z

[35] Ma, H.Y., Song, Y., Li, W., Li, C.L., 2024. Epigenetic regulation of lignin biosynthesis in wood formation. New Phytologist 241, 1128-1143. https://doi.org/10.1111/nph.20328

[36] Ma, J., Jiang, S., Kong, L., Jin, Y., Li, X., 2025. Genome-wide analysis of the caffeoyl coenzyme A-O-methyltransferase (CCoAOMT) gene family in Platycodon grandiflorus (Jacq.) A. DC. and the potential regulatory mechanism in response to copper stress. International Journal of Molecular Sciences 26, 4709. https://doi.org/10.3390/ijms26104709

[37] Ma, L., Wang, J., Qiao, K., Quan, Y., Fan, S., Wu, L., 2024. Genome-wide analysis of Caffeoyl-CoA-O-methyltransferase (CCoAOMT) family genes and the roles of GhCCoAOMT7 in lignin synthesis in cotton. Plants 13, 2983. (DOI to be added)

[38] Ma, Q.H., Zhu, H.H., Qiao, M.Y., 2018. Contribution of both lignin content and sinapyl monomer to disease resistance in tobacco. Plant Pathology 67, 642-650. https://doi.org/10.1111/ppa.12767

[39] Mamat, A., Ayup, M., Zhang, X., Gao, H., Lv, J., Li, J., 2019. Pulp lignification in Korla fragrant pear. European Journal of Horticultural Science 84, 263-273. https://doi.org/10.17660/eJHS.2019/84.5.2

[40] Mistry, J., Chuguransky, S., Williams, L., Qureshi, M., Salazar, G.A., Sonnhammer, E.L.L., Tosatto, S.C.E., Paladin, L., Raj, S., Richardson, L.J., Finn, R.D., Bateman, A., 2021. Pfam: The protein families database in 2021. Nucleic Acids Research 49, D412-D419.

869 [41] Poudel, A., Navathe, S., Chand, R., Joshi, A.K., 2019. Hydrogen peroxide prompted
870 lignification affects pathogenicity of hemi-biotrophic pathogen Bipolaris sorokiniana to
871 wheat. Plant Pathology Journal 35, 287-300.
872 [42] Qi, J., Ma, Q.G., Yang, J.M., Hou, L.Q., 2009. Characteristics of nut suture of main walnut
873 cultivars in China. Nonwood Forest Research 27, 57-61.
874 [43] Qin, Y., Jin, H.Z., Xiang, F.N., 2012. Isolation of a new caffeate O-methyltransferase (COMT)
875 gene from Chinese poplar (Populus simonii). Research on Crops 13, 577-586.
876 [44] Raes, J., Rohde, A., Christensen, J.H., Van de Peer, Y., Boerjan, W., 2003. Genome-wide
877 characterization of the lignification toolbox in Arabidopsis. Plant Physiology 133,
878 1051-1071. https://doi.org/10.1104/pp.103.026484
879 [45] Sattler, S.E., Funnell-Harris, D.L., 2013. Modifying lignin to improve bioenergy feedstocks:
880 strengthening the barrier against pathogens? Frontiers in Plant Science 4, 70.
881 https://doi.org/10.3389/fpls.2013.00070
882 [46] Shi, J.X., Zhao, H.J., Xin, D.J., Guo, Y.L., 2005. Research on walnut shelling technology
883 based on finite element analysis. Transactions of the Chinese Society of Agricultural
884 Engineering 21, 185-188.
885 [47] Sun, H.L., 2014. Cloning and functional analysis of genes related to pistil development in
886 Japanese apricot (Doctoral dissertation). Nanjing Agricultural University, Nanjing, China.
887 [48] Suo, H.M., Ni, H.H., Hu, L., Li, H.F., 2024. Genome-wide identification and analysis of the
888 CCoAOMT gene family revealed its relationship to pomegranate seed hardness. Russian
889 Journal of Genetics 60, 231-241. https://doi.org/10.1134/S1022795424020121
890 [49] Tobimatsu, Y., Wagner, A., Donaldson, L., Mitra, P., Niculaes, C., Dima, O., Kim, J.I.,
891 Anderson, N., Loqué, D., Boerjan, W., Chapple, C., Ralph, J., 2014. CCoAOMT suppression
892 modifies lignin composition in Pinus radiata. The Plant Journal 80, 1015-1026.
893 [50] Tolbert, A.K., Ma, T., Kalluri, U.C., Davison, B.H., Ragauskas, A.J., 2016. Determining the
894 syringyl/guaiacyl lignin ratio in the vessel and fiber cell walls of transgenic Populus
895 plants. Energy & Fuels 30, 5716-5720. https://doi.org/10.1021/acs.energyfuels.6b00561
896 [51] Tu, M., Wang, X., Yin, W., Wang, Y., Li, Z., Fang, L., Li, S., Wang, C., 2020. Grapevine
897 VlbZIP30 improves drought resistance by directly activating VvNAC17 and promoting

lignin biosynthesis through the regulation of three peroxidase genes. Horticulture Research 7, 150. https://doi.org/10.1038/s41438-020-00372-3

[52] Vanholme, R., Demedts, B., Morreel, K., Ralph, J., Boerjan, W., 2010. Lignin biosynthesis and structure. Plant Physiology 153, 895-905. https://doi.org/10.1104/pp.110.155119

[53] Wang, Y., Wang, T., Qi, S., Wei, C., 2024. Genome-wide identification, expression profiling, and protein interaction analysis of the CCoAOMT gene family in the tea plant (Camellia sinensis). BMC Genomics 25, 238. https://doi.org/10.1186/s12864-024-10145-8

[54] Wang, Y.J., Song, S., Zhao, Y.Y., 2025. Cloning of McCCoAOMT gene from Mandragora chinghaiensis and its expression analysis under cold stress. Journal of Qinghai University 43, 55-61.

[55] Wei, T., Tang, Y., Jia, P., Wang, X., Zhang, J., Ma, Z., 2021. A cotton lignin biosynthesis gene GhLAC4, fine-tuned by ghr-miR397 modulates plant resistance against Verticillium dahliae. Frontiers in Plant Science 12, 743795. https://doi.org/10.3389/fpls.2021.743795

[56] Wu, G.L., Liu, Y., Shen, Y.Y., Niu, J.X., 2005. Anatomical study on walnut pericarp. Chinese Journal of Eco-Agriculture 13, 104-107.

[57] Wu, Z., Wang, N., Hisano, H., Yoo, C.G., Pu, Y., Ragauskas, A.J., Dixon, R.A., Wang, Z.Y., 2019. Simultaneous regulation of F5H in COMT-RNAi transgenic switchgrass alters effects of COMT suppression on syringyl lignin biosynthesis. Plant Biotechnology Journal 17, 836-845. https://doi.org/10.1111/pbi.13019

[58] Xiao, S., Hu, Q., Shen, J., Zhang, X., Liu, C., Zhang, X., Guo, X., Zhang, X., Ye, W., 2021. GhMYB4 downregulates lignin biosynthesis and enhances cotton resistance to Verticillium dahliae. Plant Cell Reports 40, 735-751. https://doi.org/10.1007/s00299-021-02672-x

[59] Xiong, F.R., Chen, Q., Liu, Y., Chen, S.W., 2025. Preliminary study on the roles of lignin synthesis genes HCT and CCoAOMT in cassava resistance to Phenacoccus solenopsis. Chinese Journal of Tropical Crops 46, 2155-2163.

[60] Xu, J., Tao, X., Xie, Z., Zhang, S., Wu, J., 2021. PbCSE1 promotes lignification during stone cell development in pear (Pyrus bretschneideri) fruit. Scientific Reports 11, 9450. https://doi.org/10.1038/s41598-021-88825-0

926 [61] Yadav, S., Chattopadhyay, D., 2023. Lignin: the building block of defense responses to stress
927 in plants. Journal of Plant Growth Regulation 42, 7895-7914.
928 https://doi.org/10.1007/s00344-023-11027-9
929 [62] Yan, Y., Wang, P., Lu, Y., Wang, X., Zeng, H., Guo, J., He, G., Peng, M., 2021. MeRAV5
930 promotes drought stress resistance in cassava by modulating hydrogen peroxide and lignin
931 accumulation. The Plant Journal 107, 847-860. https://doi.org/10.1111/tpj.15350
932 [63] Yang, G., Peng, S., Wang, T., Ma, X., Zhang, R., Fu, X., 2021. Walnut ethylene response
933 factor JrERF2-2 interacts with JrWRKY7 to regulate the GSTs in plant drought tolerance.
934 Ecotoxicology and Environmental Safety 228, 112945.
935 https://doi.org/10.1016/j.ecoenv.2021.112945
936 [64] Ye, Z.H., Kneusel, R.E., Matern, U., Varner, J.E., 1994. An alternative methylation pathway
937 in lignin biosynthesis in Zinnia. The Plant Cell 6, 1427-1439.
938 https://doi.org/10.1105/tpc.6.10.1427
939 [65] Ye, Z.H., Varner, J.E., 1995. Differential expression of two O-methyltransferases in lignin
940 biosynthesis in Zinnia elegans. Plant Physiology 108, 459-467.
941 https://doi.org/10.1104/pp.108.2.459
942 [66] Yu, Y., Yu, Y., Cui, N., Zhang, K., Wang, Y., Sui, X., 2022. Lignin biosynthesis regulated by
943 CsCSE1 is required for Cucumis sativus defence to Podosphaera xanthii. Plant
944 Physiology and Biochemistry 186, 88-98. https://doi.org/10.1016/j.plaphy.2022.06.030
945 [67] Yusuf, C.S., Chand, R., Mishra, V.K., Joshi, A.K., 2016. The association between leaf
946 malondialdehyde and lignin content and resistance to spot blotch in wheat. Journal of
947 Phytopathology 164, 896-903. https://doi.org/10.1111/jph.12520
948 [68] Zheng H, Wang Y, Ren M, Chen J, Huang L, et al. 2025. Impact of CPPU and combined
949 CPPU-thidiazuron treatments on fruit quality and volatile compounds in 'Jinling Xiangxin'
950 grapes. Technology in Horticulture 5: e0. https://doi.org/10.48130/tihort-0025-0030
951 [69] Zhao, S.G., Zhao, Y.P., Wang, H.X., Han, H.J., 2011. Influencing factors of walnut nut shell
952 structure. Scientia Silvae Sinicae 47, 70-75.
953 [70] Zhao, X., Li, P., Li, C., Qu, G., Wang, S., Yang, C., 2022. The key regulators and metabolic
954 intermediates of lignin response to low temperatures revealed by transcript and targeted

metabolic profiling analysis in poplar. Agronomy 12, 2506. https://doi.org/10.3390/agronomy12102506

[71] Zhao, Y.P., Zhao, S.G., Wang, H.X., Han, H.J., 2007. Relationship between walnut shell structure and commercial quality of kernel. Scientia Silvae Sinicae 43, 81-85.

[72] Zhong, R., Morrison, W.H. III, Negrel, J., Ye, Z.H., 1998. Dual methylation pathways in lignin biosynthesis. The Plant Cell 10, 2033-2046. https://doi.org/10.1105/tpc.10.12.2033

Supplementary Files

This is a list of supplementary files associated with this preprint. Click to download.

- SupplementaryFigureS1.jpg